Environmental Science & Technology

Article

Cite This: Environ. Sci. Technol. 2019, 53, 1585−1594

pubs.acs.org/est

Protection Mechanisms of Periphytic Biofilm to Photocatalytic Nanoparticle Exposure

Ningyuan Zhu,[†,#,▽] Sichu Wang,[†,▽] Cilai Tang,[‡] Pengfei Duan,[§] Lunguang Yao,[§] Jun Tang,[*,†,▽] Po Keung Wong,[∥] Taicheng An,[⊥] Dionysios D. Dionysiou,[#] and Yonghong Wu[†]

[†]Zigui Ecological Station for Three Gorges Dam Project, State Key Laboratory of Soil and Sustainable Agriculture, Institute of Soil Sciences, Chinese Academy of Sciences, 71 East Beijing Road, Nanjing 210008, China

[‡]College of Hydraulic & Environmental Engineering, China Three Gorges University, Yichang 443002, China

[§]Collaborative Innovation Center of Water Security for Water Source, Region of Mid-line of South-to-North Diversion Project, Nanyang Normal University, Nanyang 473061, China

[∥]School of Life Sciences, The Chinese University of Hong Kong, Shatin, NT Hong Kong SAR, China

[⊥]Guangzhou Key Laboratory of Environmental Catalysis and Pollution Control, School of Environmental Science and Engineering, Institute of Environmental Health and Pollution Control, Guangdong University of Technology, Guangzhou 510006, China

[#]Department of Chemical and Environmental Engineering (ChEE), 705 Engineering Research Center, University of Cincinnati, Cincinnati, Ohio 45221-0012, United States

[▽]College of Resource and Environment, University of Chinese Academy of Sciences, Beijing 100049, China

Supporting Information

ABSTRACT: Researchers are devoting great effort to combine photocatalytic nanoparticles (PNPs) with biological processes to create efficient environmental purification technologies (i.e., intimately coupled photobiocatalysis). However, little information is available to illuminate the responses of multispecies microbial aggregates against PNP exposure. Periphytic biofilm, as a model multispecies microbial aggregate, was exposed to three different PNPs (CdS, TiO_2, and Fe_2O_3) under xenon lamp irradiation. There were no obvious toxic effects of PNP exposure on periphytic biofilm as biomass, chlorophyll content, and ATPase activity were not negatively impacted. Enhanced production of extracellular polymetric substances (EPS) is the most important protection mechanism of periphytic biofilm against PNPs exposure. Although PNP exposure produced extracellular superoxide radicals and caused intracellular reactive oxygen species (ROS) accumulation in periphytic biofilm, the interaction between EPS and PNPs could mitigate production of ROS while superoxide dismutase could alleviate biotic ROS accumulation in periphytic biofilm. The periphytic biofilms changed their community composition in the presence of PNPs by increasing the relative abundance of phototrophic and high nutrient metabolic microorganisms (families Chlamydomonadaceae, Cyanobacteriacea, Sphingobacteriales, and Xanthomonadaceae). This study provides insight into the protection mechanisms of microbial aggregates against simultaneous photogenerated and nanoparticle toxicity from PNPs.

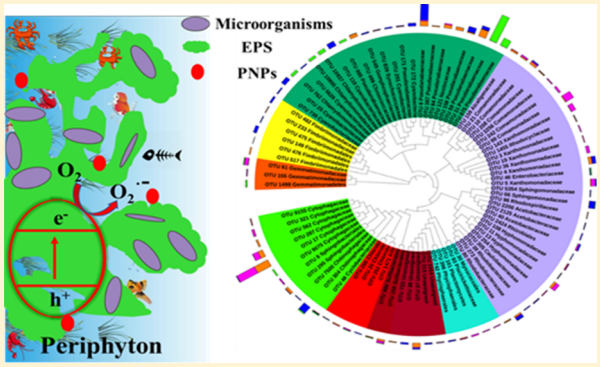

INTRODUCTION

Processes based on photocatalyst nanoparticles (PNPs) are playing critical roles in several fields including disinfection of bacteria,[1] energy harvesting,[2] electrochemical reactions,[3] and environmental remediation via advanced oxidation/reduction processes (AO/RP).[4] Researchers also exploit strategies to combine PNP based technology with biological processes (i.e., intimately coupled photobiocatalysis) to improve contaminant removal efficiency.[5] However, the biological compatibility of PNPs must be taken into consideration to avoid microorganisms being attacked or killed.[5−7] CdS, TiO_2, and Fe_2O_3 PNPs have shown great application potential in combination with various biological processes,[8,9] such as ammonia synthesis from nitrogen,[10] removal of organic pollutants in wastewater,[5] and microbial photoelectrochemical system.[7] Due to large-scale uses, it is necessary to investigate their potential environmental impacts and possible effects on biological systems under sunlight irradiation.

Received: September 2, 2018
Revised: January 4, 2019
Accepted: January 7, 2019
Published: January 7, 2019

DOI: 10.1021/acs.est.8b04923
Environ. Sci. Technol. 2019, 53, 1585−1594

Traditionally, PNPs have been investigated in disinfection of single species microorganisms or biofilm including bacteria (*E. coli*[11]), fungi (*Fusarium* sp.[12]) and algae (*Microcystis aeruginosa*[13]) under sunlight illumination. These studies confirmed the antimicrobial mechanisms of PNPs on single species microorganisms or simple microbial communities, including DNA damage, oxidative stress by reactive oxygen species (such as superoxide radicals and hydroxyl radicals), or membrane destruction. Recently, researchers have started to investigate the toxic effects of nanoparticles (including PNPs) on multispecies microbial aggregates that are the form of most microorganisms in nature.[1,14−16]

Periphytic biofilm, a typical microbial aggregate in aquatic ecosystem (such waterways in paddy fields and wetland), has a complex community composition, a complete food chain, and abundant EPS.[17] Periphytic biofilms have been demonstrated to play a major role in the environmental behaviors of nanoparticles (NPs) in environmental systems, including NP accumulation,[18] biotransformation,[19] and transfer through food chain.[20] The characteristics of microbial aggregates, such as complex community composition and abundant EPS, could also result in complex responses to NPs for periphytic biofilm which is different from the study on single species populations.[15,21−23] Periphytic biofilm display versatile responses (including enzyme activity, production of extracellular polymeric substances (EPS), photosynthesis) to NP (Ag, Fe_2O_3, and CeO_2) or heavy metal ion (Cd^{2-}, As^{3-}, and Pb^{2+}) intrusion.[15,21,24] Multispecies microbial aggregates constantly adapt their population fitness to increase their tolerance to NPs through their complex population structure and corresponding interspecies interactions.[15,25,26] When exposed to TiO_2, Ag, and CeO_2 NPs, multispecies microbial aggregates showed significant increases in the α diversity of bacterial communities.[16,22,27] Our previous studies focused on the responses of periphytic biofilm to NP exposure demonstrating the important role of EPS in defending against nanotoxicity.[15,22]

Although these studies have demonstrated the responses of multispecies microbial aggregates (e.g., periphytic biofilm) to NP exposure from a physiological and ecological view, there is little information about the relationship between biological responses and protection mechanisms against exposure to NPs (e.g., PNPs). Compared with other NPs, PNPs can induce more oxidative stress to microorganisms due to their photoresponses under suitable wavelengths of light irradiation.[28] Numerous studies have correlated the band gaps of metal oxide NPs to their capacity to generate oxidative stress[29,30] and thus toxicity to cells.[31,32] However, little information is available to evaluate the influence of the band gaps of PNPs on their toxicities to multispecies microbial aggregates (periphytic biofilm) under light irradiation. Most importantly, how the multispecies microbial aggregate (periphytic biofilm) protects itself from the stress of PNP exposure remains unclear.

In this study, TiO_2, CdS, and Fe_2O_3 PNPs were chosen to evaluate their toxic effect on periphytic biofilm. The objectives of this study were to (i) explore the distribution of PNPs in the periphytic biofilm matrix, (ii) evaluate the influence of PNPs on periphytic biofilm, and (iii) explore the protection mechanisms of periphytic biofilm in defending against PNPs exposure. This study is expected to provide new insight into the protection mechanisms of multispecies microbial aggregates against PNPs.

MATERIALS AND METHODS

Preparation of Periphytic Biofilm and PNP Suspensions. Periphytic biofilm, originated from Xuanwu Lake, Nanjing, China, was inoculated into our biofilm culture systems with WC medium (see Supporting Information).[21] CdS, TiO_2, and Fe_2O_3 PNPs (uncoated) used in this study were purchased from Aladdin, China. The primary particle sizes based on TEM images of CdS and TiO_2 PNPs were 36.7 ± 3.5 nm and 42.6 ± 5.8 nm, while the width and length of Fe_2O_3 PNPs were 9.9 ± 0.6 nm and 72.4 ± 7.5 nm, respectively. The stock solutions of individual PNPs were prepared by adding 100 mg of respective PNPs to 100 mL deionized water, shaking vigorously under ultrasonic treatment (300 W, 100 Hz) for 30 min, and then diluting to 1000 mL in a volumetric flask. Before preparing the stock solution of PNPs, the PNPs were sterilized using UV irradiation (low-pressure UV lamp, UVC15W/T8, CREATOR, China) for 1 h in clean benches. The distilled water for solution preparation was sterilized by autoclave sterilization. All the experimental operations for solution preparation before sealing were carried out under sterilized conditions.

Periphytic Biofilm Exposure to PNPs. The 14 day old periphytic biofilms were exposed to PNP suspensions for 7 days (for exposure concentration of PNPs, see Supporting Information, Table S1). The 7 day period was based on a 21 day periphytic biofilm lifecycle according to our previous study.[33] Periphytic biofilm was collected from our biofilm culture systems by a sterilized silicone spatula for the following experiments. All the periphytic biofilms were washed three times using sterilized 0.9% NaCl solution and centrifuged before each experiment. Then, 20, 50, and 500 mL of PNP stock solution and 1 mL WC media stock solution (1000 times concentration of the culture medium) were put in 1000 mL volumetric flasks and diluted by distilled water to obtain the final required final concentration of PNPs (see Supporting Information, Table S1). Then the required concentration PNP solutions containing WC medium were obtained, and 50 mL of the PNP solutions were added into 150 mL flasks. Then 1.0 g of the periphytic biofilm (after centrifugation) was added into every flask. The control flask contained no PNPs. All flasks were then sealed with sterilized parafilm to allow for gas exchange and placed in an incubation room with a standard light−dark cycle of 12 h/12 h (xenon lamp, 150 W) at 28 ± 1 °C. Both the control and each treatment consisted of six replicates. After a 7 day exposure, the biomass, concentration of chlorophyll, and EPS productivity were measured to evaluate the influence of the PNPs on periphytic biofilm growth. The analytical methods to measure biomass, concentration of total chlorophyll content, and EPS were detailed in Supporting Information.

Characteristics of EPS and PNPs. Two EPS extraction methods were adopted to evaluate productivity of EPS and content of metals in the EPS and prepare periphytic biofilm samples for the ROS accumulation experiments (details provided in Supporting Information). To determine the distribution of PNPs in periphytic biofilm system, metal content in different fractions (metals in solution, loosely bound metals, and irreversibly bound metals) were detected by ICP-MS (7700x-JP12502215, Agilent Technologies, USA) (details provided in Supporting Information). Electron spin resonance (ESR) analysis (EMX 10/12, Bruker, Germany) was performed to detect the ROS spectra in the PNPs/EPS system

DOI: 10.1021/acs.est.8b04923
Environ. Sci. Technol. 2019, 53, 1585−1594

under xenon lamp irradiation (see Supporting Information). The morphologies of PNPs were investigated using transmission electron microscope (TEM, Zeiss 900, Carl Zeiss, Germany) operating at 200 kV after exposure to WC medium and EPS. Hydrodynamic diameters of PNPs in WC medium or EPS extracted from periphytic biofilm were measured using a Zetasizer (90PLUS PALS, NanoBrook, USA). The components of PNPs were determined using X-ray diffraction (XRD) (LabX, XRD-6100, Japan) with Cu Kα radiation (λ = 1.54056 nm) at a power of 40 keV × 30 mA. The XRD data were recorded with 2θ varying from 20° to 60° at counting time of 10 s and a scanning mode with a step size of 0.02°.

Characteristics of Periphytic Biofilm. The production of reactive oxygen species (ROS) by periphytic biofilm caused by PNPs in the presence and absence of EPS was also detected. The superoxide dismutase (SOD) activity and adenosine triphosphatase (ATPase) activity were measured to evaluate the response of the periphytic biofilm to PNPs exposure. The distribution of PNPs in the periphytic biofilm matrix was also studied using scanning electron microscopy coupled with energy dispersive X-ray spectroscopy (SEM, JEOL Co, Ltd., Japan; EDX, Oxford Instruments, UK) and TEM (Zeiss 900, Carl Zeiss, Germany). To evaluate the influence of PNPs on community composition and diversity of periphytic biofilm, high-throughput sequencing of the 16S rDNA gene of periphytic biofilm was also performed. All the detailed methods are provided in Supporting Information.

Statistics. Principal component analysis (PCA)[34] was used to analyze the genus-level OTU-table from high-throughput sequencing to investigate variation of community composition of periphytic biofilm in the presence of PNPs. The detected biological and phycological parameters of periphytic biofilm (productivity of EPS, activities of ATPase and SOD, concentrations of ROSs and chlorophyll, and distribution of PNPs in solution or in EPS) were used as the matrix for canonical correspondence analysis (CCA) to distinguish their relationships with community composition of periphytic biofilm (represented by the genus-level OTU-table). PCA and CCA were calculated in the vegan package by R software. The *t*-tests were used to evaluate whether the differences between the treatments and control were statistically significant, unless otherwise specified. The probability *p* value was set at 0.05 level for all analyses. All figures were prepared using Origin 9.0 software.

RESULTS

Characteristics of Photocatalytic Nanoparticles. The XRD patterns showed the existence of CdS with hexagonal phase which was demonstrated by diffraction peaks at 2θ = 26.74, 43.84, and 52.38 degrees (Figure S1A). TiO_2 crystals with the anatase phase were proved by the diffraction peaks at 25.40, 37.96, 48.16, 54.10, and 55.23 (Figure S1B). The α-Fe_2O_3 crystal was confirmed by the diffraction peaks at 33.24, 35.77, 40.89, and 54.16 for Fe_2O_3 PNPs (Figure S1 C).

The TEM images and the corresponding primary particle sizes of PNPs in WC medium and EPS are showed in Figure S2. Results showed that no statistically significant change (p > 0.05) was observed in primary particle size between PNPs in WC medium and EPS. If the primary particle size of PNPs is consistent regardless of the media used, the change of hydrodynamic diameters (AHD) could reflect the aggregation tendency of PNPs.[35] The AHD of PNPs were 53.5 ± 9.8, 61.4 ± 8.1, and 76.3 ± 10.5 nm for CdS, TiO_2, and Fe_2O_3 in WC medium, respectively (Table S2). In the presence of EPS extracted from periphytic biofilm, the AHD of PNPs were 46.7 ± 8.5, 52.2 ± 7.7, and 68.1 ± 12.4 nm for CdS, TiO_2, and Fe_2O_3, respectively. There was also no significant difference (p > 0.05) in the hydrodynamic diameters between PNPs in WC medium and EPS. Therefore, combining with EPS did not show a significant influence on the aggregation of the PNPs.

Photocatalytic materials can produce reactive oxygen species ($^{\bullet}OH$ and $O_2^{\bullet-}$) under suitable light irradiation which may pose oxidative stress on microorganisms.[5,36] ESR tests demonstrated the presence of $O_2^{\bullet-}$ represented by the three-line signal remaining the same proportionately in the CdS/EPS and TiO_2/EPS systems under Xe-lamp irradiation (Figure 1)

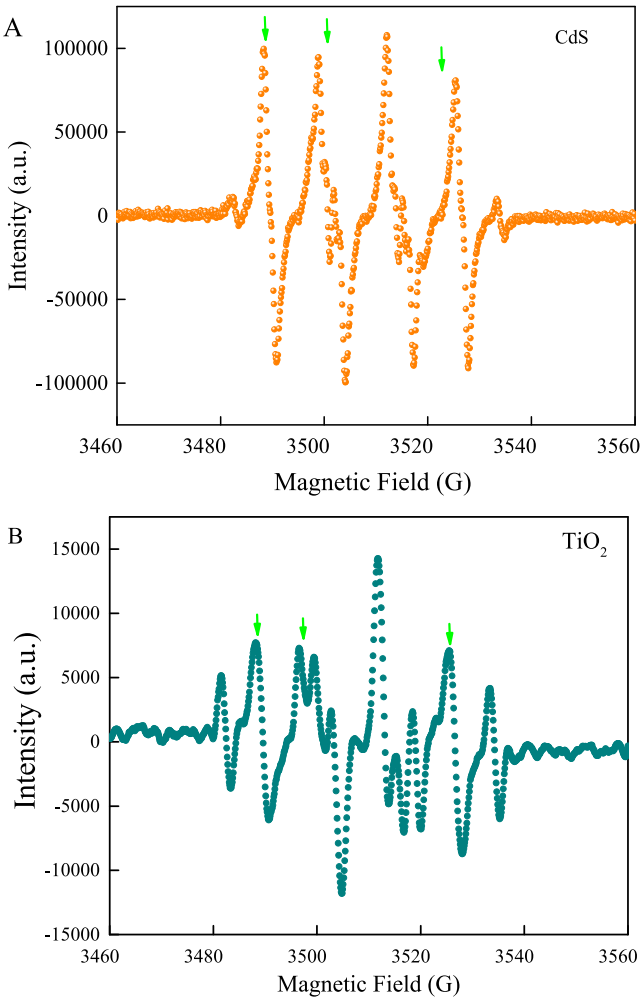

Figure 1. ESR spectra of (A) TEMP $O_2^{\bullet-}$ adducts in CdS−EPS systems irradiated for 1 min. (B) TEMP $O_2^{\bullet-}$ adducts in TiO_2−EPS systems irradiated for 1 min.

.[37] There was no $^{\bullet}OH$ detected in any PNPs/EPS systems. Therefore, $O_2^{\bullet-}$ might be the main ROS produced in the PNPs/EPS system. It should be noted that neither $^{\bullet}OH$ nor $O_2^{\bullet-}$ was detected in Fe_2O_3/EPS system (data not shown). However, Fe_2O_3 PNPs have been well demonstrated as photoresponse materials under suitable light irradiation (i.e., natural sunlight), which could pose oxidative stress on microorganisms.[38] The low response to the stimulated sunlight irradiation or the low position of the conduction band may be

DOI: 10.1021/acs.est.8b04923
Environ. Sci. Technol. 2019, 53, 1585−1594

the reason for the undetectable ROS in the Fe_2O_3/EPS system.[39]

Biological and Physiological Effects on Periphytic Biofilm. The biomasses of periphytic biofilms were weighed after a 7 day exposure to evaluate the growth of periphytic biofilm in the presence of PNPs (Table 1). The average biomass in the control was 1.45 g after a 7 day cultivation. Biomasses were not statistically different ($p > 0.05$) in the presence of TiO_2 (ranging from 1.55 ± 0.14 to 1.3 ± 0.06 g, $p > 0.05$) or Fe_2O_3 (ranging from 1.56 ± 0.09 to 1.37 ± 0.05 g, $p > 0.05$) and 2 mg L^{-1} of CdS (1.42 ± 0.13, $p > 0.05$). The presence of 5 mg L^{-1} CdS was beneficial to the growth of periphytic biofilm as the biomass increased to 1.86 g which was significantly higher ($p < 0.05$) than that in the control. However, the presence 50 mg L^{-1} of CdS was unfavorable to periphytic biofilm growth as the biomass significantly decreased to 0.96 g ($p < 0.05$).

Table 1. Biomass (g), Chlorophyll (mg g^{-1}), and Total EPS (mg L^{-1}) Productivity of Periphytic Biofilm in the Control and after Exposure to PNPs (CdS, TiO_2, and Fe_2O_3)[c]

treatments		biomass (g)	chlorophyll (mg g^{-1})	EPS (mg L^{-1})
control		1.45 ± 0.07	2.7 ± 0.2	70 ± 6
CdS	2	1.42 ± 0.13 [a]	2.6 ± 0.1 [a]	81 ± 4 [a]
	5	1.86 ± 0.08 [b]	2.4 ± 0.3 [a]	116 ± 7 [b]
	50	0.96 ± 0.12 [b]	1.2 ± 0.1 [b]	42 ± 3 [b]
TiO_2	2	1.55 ± 0.14 [a]	2.8 ± 0.4 [a]	77 ± 6 [a]
	5	1.47 ± 0.11 [a]	2.6 ± 0.2 [a]	103 ± 9 [b]
	50	1.30 ± 0.06 [a]	2.5 ± 0.2 [a]	102 ± 8 [b]
Fe_2O_3	2	1.51 ± 0.15 [a]	2.5 ± 0.2 [a]	75 ± 7 [a]
	5	1.56 ± 0.09 [a]	2.8 ± 0.3 [a]	94 ± 5 [b]
	50	1.37 ± 0.05 [a]	2.3 ± 0.3 [a]	107 ± 8 [b]

[c]Mean value ± SD; $n = 3$. All the statistical significance between each treatment and control were calculated by *t*-test. The a represents nonsignificance between treatment and control ($p > 0.05$) while the b represents statistical significance between treatment and control ($p < 0.05$).

The concentration of chlorophyll content was calculated to reflect the growing condition of the photosynthetic microorganisms (cornerstone species in periphytic biofilm) in the periphytic biofilm. Only high concentrations of CdS (>5 mg L^{-1}) significantly decreased the chlorophyll content in comparison to the control ($p < 0.05$) while TiO_2 and Fe_2O_3 and low CdS concentration did not produce a statistical difference ($p > 0.05$) in the concentration of chlorophyll content of periphytic biofilm (Table 1). The total production of EPS in the presence of the different PNPs is presented in Table 1. The presence of CdS (low concentration), TiO_2, and Fe_2O_3 facilitated production of EPS. In particular, TiO_2 and Fe_2O_3 (>2 mg L^{-1}) and low concentration of CdS (2 and 5 mg L^{-1}) significantly increased the productivity of EPS ($p < 0.05$). The intracellular protein content of periphytic biofilm between control and PNP treatments was not statistically different ($p > 0.05$), indicating that the increased EPS productivity was unlikely to be attributed to the increasing of cell numbers in periphytic biofilm (Figure S3).[40] This result was consistent with previous studies, which also observed excessive production of EPS as a main response of microbial aggregates exposed to metal contaminations, especially for nanoparticles.[15,17,24] However, the total amount of EPS significantly decreased in the presence of high concentrations of CdS (>5 mg L^{-1}) compared to the control ($p < 0.01$).

The presence of PNPs often causes accumulation of reactive oxygen species (ROS) in microorganisms because PNPs have been proven to produce radical species, such as hydroxyl radicals ($^{\bullet}OH$) and superoxide radicals ($O_2^{\bullet-}$), which cause strong oxidative stress to microorganisms.[5,41] The presence of CdS, TiO_2, and Fe_2O_3 resulted in significantly increased ROS accumulation of 160.3% ($p < 0.01$), 145.7% ($p < 0.01$), and 125.0% ($p < 0.05$), respectively, compared to the control in the presence of EPS (Figure 2A). The ROS accumulation was then detected after EPS removal from periphytic biofilm using heat treatment. The ROS accumulation significantly ($p < 0.01$) increased by 374.1%, 336.5%, and 194.3% for CdS, TiO_2, and Fe_2O_3, respectively, compared to the control in the absence of EPS. Results also showed that heat treatment did not cause any significant difference in ROS accumulation in periphytic

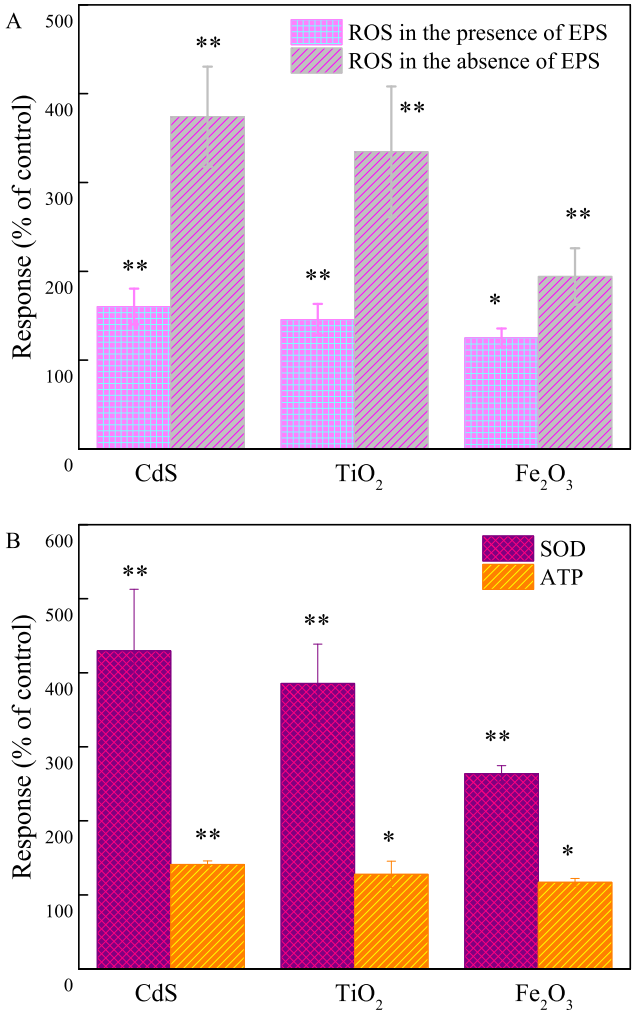

Figure 2. (A) Effects of photocatalytic nanoparticles on reactive oxygen species (ROS) accumulation of periphytic biofilm in the presence and absence of EPS. (B) Activity of superoxide dismutase (SOD) and ATPase of periphytic biofilm in the presence of photocatalytic nanoparticles (PNPs) compared to the control. ** and * represented the high significant difference ($p < 0.01$) and significant difference ($p < 0.05$) between treatment and control based on *t* test, respectively. The concentration of CdS, TiO_2, and Fe_2O_3 was 5 mg L^{-1}.

DOI: 10.1021/acs.est.8b04923
Environ. Sci. Technol. 2019, 53, 1585−1594

Table 2. α Diversity Parameters from the Results of the MiSeq Sequencing[a]

treatment	observed species	Chao1	Shannon	Simpson
control	959 ± 42	1495.40 ± 55.55	6.17 ± 0.13	0.94 ± 0.01
CdS	686 ± 29	1097.28 ± 29.62	5.15 ± 0.09	0.88 ± 0.01
TiO_2	868 ± 42	1352.47 ± 158.50	5.49 ± 0.54	0.90 ± 0.06
Fe_2O_3	708 ± 48	1036.6 ± 77.7	5.72 ± 0.25	0.94 ± 0.02

[a]Mean value ± SD; n = 3. Chao 1 is an index that was reported by Chao first which was used for nonparametric estimation of the number of classes in a population.

biofilm (Figure S4) and the presence of PNPs did not likely affect fluorescence measurement (Figure S4). Therefore, EPS may help mitigate ROS attacks of PNPs to protect microorganisms in periphytic biofilm matrices.

SOD is the key enzyme to mitigate attacks from ROS and is produced because of the oxidative stress caused by adverse environmental conditions.[42−44] The SOD activity increased significantly in the CdS (429.5% higher than the control, $p < 0.01$), TiO_2 (385.4% higher than the control, $p < 0.01$), and Fe_2O_3 (263.6% higher than the control $p < 0.01$) treatments (Figure 2B). The metabolic activity of microorganisms (represented by activity of ATPase) in periphytic biofilm was then evaluated.[45] The activity of ATPase was significantly enhanced in the presence of CdS, TiO_2, and Fe_2O_3 (increased by 141.0% ($p < 0.01$), 127.7% ($p < 0.05$), and 116.9% ($p < 0.05$), respectively) (Figure 2B). According to biological and phycological parameters, periphytic biofilm could still maintain its growth with CdS (2 and 5 mg L^{-1}), TiO_2, and Fe_2O_3 PNPs.

Diversity and Community Composition of Periphytic Biofilm in the Presence of PNPs. The diversity of microorganisms in periphytic biofilm was analyzed by MiSeq sequencing technology. Results showed that exposure to TiO_2 and CdS had negative impacts on all α diversity (Shannon, Simpson indices) and richness indices (observed species, Chao 1) of periphytic biofilm ($p < 0.05$) compared to the control (Table 2). Thus, TiO_2 and CdS PNPs had a significant negative effect on the microbial diversity of periphytic biofilm. Interestingly, the presence of Fe_2O_3 significantly decreased the richness (observed species and Chao 1 indices, $p < 0.05$) of periphytic biofilm but did not significantly affect the α diversity (Shannon and Simpson indices, $p > 0.05$). Therefore, Fe_2O_3 PNPs showed a relatively small inhibition on the diversity of community in periphytic biofilm compared to TiO_2 and CdS NPs. The Simpson index is more sensitive to evenness, and the Shannon index is more sensitive to richness. For all the three PNPs, Shannon indices showed a greater decline than Simpson indices, indicating that PNP exposure induced a more negative effect on the richness of community in periphytic biofilm while having a lower influence on the evenness of community.

Changing the community composition of different populations in multispecies microbial aggregates is an effective strategy to protect a microbial community against unfavorable environmental stress and enable adaptation to new environments. In the presence of PNPs, the composition of the periphytic biofilms changed dramatically (Figure 3A). Periphytic biofilms in the control and treatments were mainly composed of phyla Proteobacteria, Cyanobacteria, Bacteroidetes, Armatimonadetes, and Planctomycetes. The detected main community of periphytic biofilm in phyla level was consistent with former studies.[15,22] When CdS was present, the relative abundance of Cyanobacteria and Armatimonadetes decreased significantly while Proteobacteria was almost two times more abundant than that in the control. The presence of

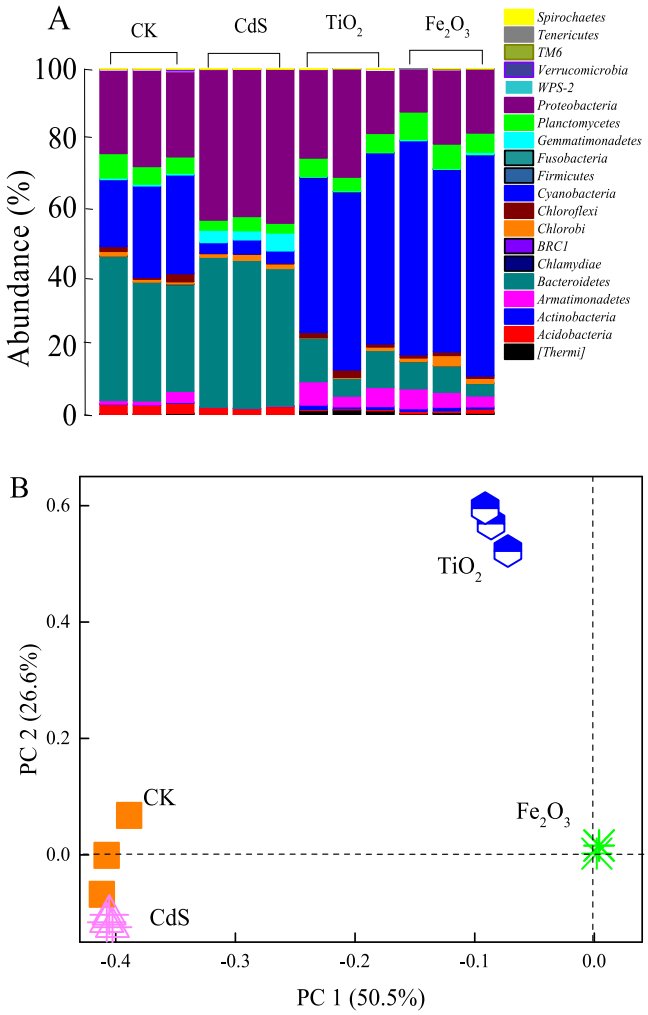

Figure 3. (A) Phylum level community composition of bacteria in periphytic biofilm. (B) Principal component analysis (PCA) output of bacterial communities in periphytic biofilm exposed to different PNPs. Numbers in parentheses indicate percent variation explained by the first principal component (PC 1) and the second principal component (PC 2). CK = control. The concentration of PNPs was: CdS = 5 mg L^{-1}, TiO_2 = 5 mg L^{-1}, Fe_2O_3 = 5 mg L^{-1}.

TiO_2 and Fe_2O_3 promoted an increase in Cyanobacteria but caused a decrease in Proteobacteria. PCA was used to investigate community composition of the periphytic biofilm in the presence of the different PNPs. PCA results showed significant variation in community composition of periphytic biofilm between the control and PNPs treatments (represented by the spatial distribution of samples in Figure 3B). Therefore, periphytic biofilm possesses the ability to change its community composition to protect microorganisms against PNPs (i.e., CdS, TiO_2, and Fe_2O_3) exposure.

DOI: 10.1021/acs.est.8b04923
Environ. Sci. Technol. 2019, 53, 1585−1594

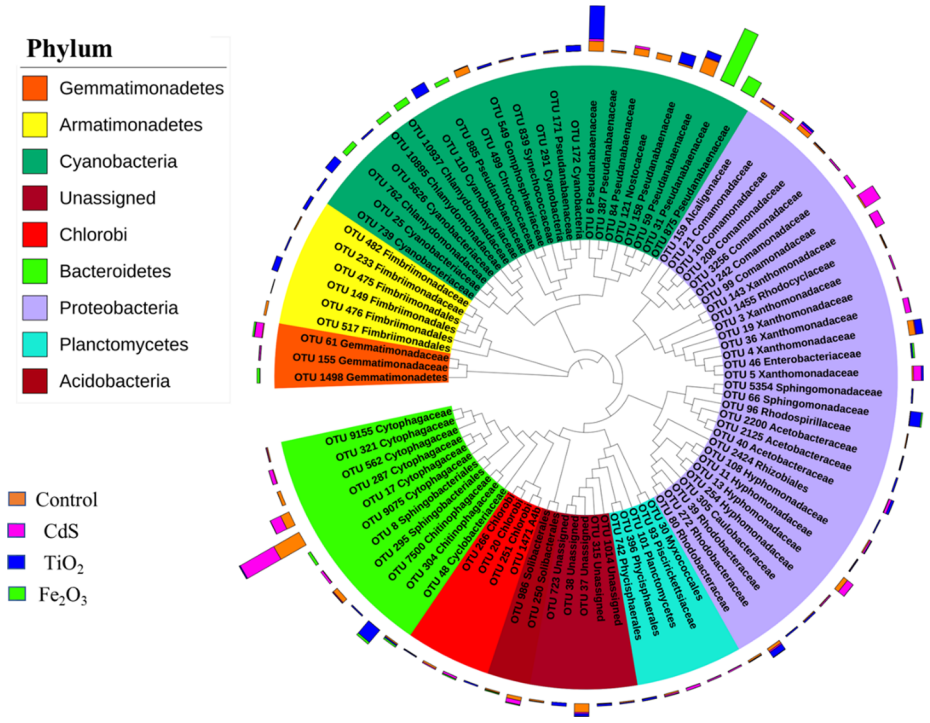

Figure 4. Circular phylogenetic tree based on OTU representative sequences of bacteria detected in all periphytic biofilm samples. The bars in the outer band represent the OTU numbers. The concentration of PNPs was: CdS = 5 mg L^{-1}, TiO_2 = 5 mg L^{-1}, Fe_2O_3 = 5 mg L^{-1}.

A phylogenetic tree of 88 types of bacteria in periphytic biofilm was constructed using MEGA 5 (Figure 4). Results show the relative abundance of families Sphingobacteriales, Xanthomonadaceae, and Hyphomonadaceae (phylum Proteobacteria), and families Cytophagaceae and Chitinophagaceae (phylum Bacteroidetes) increased in the CdS treatment compared to the control. The relative abundance of families Chlamydomonadaceae and Cyanobacteriaceae (phylum Cyanobacteria) increased significantly in the TiO_2 or Fe_2O_3 treatment ($p < 0.05$) compared to the control. Although the presence of PNPs had no statistically different influence ($p > 0.05$) on periphytic biofilm diversity, the relative abundance of beneficial populations increased in periphytic biofilm (phototrophic and high nutrient metabolic microorganisms such as families Chlamydomonadaceae, Cyanobacteriacea, Sphingobacteriales, and Xanthomonadaceae). Furthermore, these microorganisms may use the photogenerated electrons from PNPs to accelerate their N-metabolism or have a high primary productivity which is also beneficial for a higher productivity of EPS,[22,46,47] and improvement in the activity of related enzymes such as CAT and SOD.[22,24] The higher productivity of EPS and enzyme activity was helpful for periphytic biofilm exposed to PNPs.[22,23]

Interaction between EPS and PNPs. The distribution forms of PNPs in biological systems are closely related to toxic responses of microorganisms to PNPs.[48] To further distinguish the distribution forms of PNPs in periphytic biofilm matrices, the concentrations of PNPs in ion or particle form in solution or embedded in EPS were determined after cultivation experiments. There are few ionic forms of Cd, Ti, and Fe (6, 2, and 3 $\mu g\ L^{-1}$, respectively) present in solution (Figure S5). The loosely bound and irreversibly bound forms of PNPs were present in EPS. There were few loosely bound forms of PNPs (70, 40, and 110 $\mu g\ L^{-1}$ for CdS, TiO_2, and Fe_2O_3, respectively). Thus, TiO_2, CdS, and Fe_2O_3 were mainly distributed in EPS in the irreversibly bound forms.

SEM-EDS images showed that the presence of PNPs affected the morphology of the periphytic biofilm surface (Figure S6). A loose and porous biofilm structure was observed in the control. The morphology then changed to rough with some particle distribution in the presence of TiO_2 and Fe_2O_3. The periphytic biofilm exhibited a compact morphology with particle distribution in the presence of CdS. Further EDS spectra demonstrated that Ti (1.53%, wt %), Fe (2.16%, wt %), and Cd (1.02%, wt %) were distributed in the periphytic biofilm after exposure to TiO_2, CdS, and Fe_2O_3, respectively (Figure S6). An SEM-EDS test was also used to scan the cross-section of periphytic biofilm (Figure S7). Results showed that no Cd, Ti, or Fe were observed in the cross-sections of periphytic biofilm in PNPs treatments. These results indicated that PNPs affected the morphology of the periphytic biofilm; TiO_2, CdS, and Fe_2O_3 were mainly distributed on the surface of the periphytic biofilm matrix. TEM images showed no obvious particles in the control periphytic biofilm (Figure S8). TiO_2, Fe_2O_3, and CdS were distributed on the external surface of cells, and some particles were aggregated (Figure S8). Compared to Figure S2C,F, the morphology of Fe_2O_3 changed in the periphytic biofilm, which indicates that microorganisms in periphytic biofilm may change the morphology of Fe_2O_3.

DISCUSSION

Many researchers have endeavored to evaluate the nanotoxicity of engineered nanoparticles (including PNPs) to individual cells and single/multispecies aggregates.[49−51] The hypotheses were related to how nanoparticles result in toxicity to the organisms involved in the transportation of nanoparticles in biofilm matrices (result in the release of heavy metal ions, intact with cells or endocytosis potential by cells).[52,53] PNPs

DOI: 10.1021/acs.est.8b04923
Environ. Sci. Technol. 2019, 53, 1585−1594

could also pose threats to microorganisms due to ROS attack.[54,55] While traditional studies on nanotoxicity and multispecies microbial aggregates marked a step forward in understanding the response of microorganisms to nanoparticles,[5,15,27] the protection mechanisms of multispecies aggregates against intrusion of nanoparticles remained unclear. This study presented a systemic examination of this issue.

Multispecies microbial aggregates can protect cells against unfavorable environments because of the interdependencies and convoluted intraspecific and interspecific networks that are beneficial to detoxification and reduction of ROS.[56] Periphytic biofilm, as a typical autotropic multispecies microbial aggregate, enhanced productivity of EPS to protect microorganisms against intrusion of PNPs. Unlike the toxicity of nanoparticles to single species microorganisms, the presence of nanoparticles can affect many aspects of multispecies microbial aggregates including biomass,[15] metabolic activity (e.g., enzyme activity, photosynthesis),[22] and EPS productivity.[17] Thus, multispecies microbial aggregates show changes in community composition to adapt to the presence of nanoparticles.[16] CCA was used to evaluate the influence of seven factors (EPS productivity, ATPase, SOD, ROS, concentration of chlorophyll, and distribution of PNPs in solution or in EPS) on community composition of periphytic biofilm. CCA results showed that EPS productivity played the most important role in community composition of periphytic biofilm (Figure S9). The second most important factor is distribution of PNPs in EPS.

EPS played an important role in protecting cells against adverse environments. EPS not only interacted with nanoparticles but also affected their aggregation tendency and distribution forms.[22,35] EPS could interact with PNPs through adsorption processes over a short period: PNPs showed a fitted pseudo second kinetic model to adsorption of EPS (Figure S10), which indicated that adsorption of EPS by PNPs was mainly due to chemical adsorption.[21,57] Previous studies had proved the existence of abundant functional groups in EPS, such as amino, hydroxyl, and carbonyl, which may facilitate PNP adsorption of EPS by formation of hydrogen bonds.[17,58] The adsorbed EPS inevitably influenced the aggregation tendency and distribution of nanoparticles which is an important factor in toxicity to microorganisms.[35,58] SEM-EDS (Figure S6 and Figure S7) and TEM (Figure S8) images of periphytic biofilm further proved that the interaction of PNPs with EPS affected the distribution of PNPs in periphytic biofilm. Thus, periphytic biofilm could produce more EPS to maintain PNPs in the surface which enabled biofilm cells to resist PNP further intrusion to the cells.

PNPs could also cause oxidative stress on periphytic biofilm which causes accumulated ROS. ROS generation of photocatalysts was dependent on whether their position of the conduction band (Ec) was located within the range of cellular redox potential (CRP; −4.12 to −4.84 eV vs NHE).[59] The Ec values of CdS (around −4.70 eV vs NHE[60,61]) and TiO_2 (around −4.16 eV vs NHE[29]) were positioned within the CRP which could pose strong oxidative stress through generation of $O_2^{\bullet-}$ to periphytic biofilm. The Ec of Fe_2O_3 (around −4.99 eV vs NHE[29]) was out of CRP, suggesting that $O_2^{\bullet-}$ was unlikely to originate from photoresponse of Fe_2O_3. Interestingly, the biodissolution of nanoparticles in aquatic environments was involved with toxicity to microorganisms.[19] The Fe ions had been detected (Figure S5) which may cause oxidative stress on periphytic biofilm through Fenton like reactions.[62] ROS accumulation could also occur due to the disruption of metal homeostasis.[15] Fortunately, periphytic biofilms also possess the ability to protect microorganisms from ROS attack. On the one hand, periphytic biofilm enhanced SOD activity in the presence of PNPs to alleviate biotic ROS attack. The strong positive correlation between EPS productivity and SOD activity was observed (Figure S11), indicating that the presence of EPS was beneficial to maintain enzymatic activity.[63,64] On the other hand, the EPS also played an important role in mitigating biotic/abiotic ROS attack which relieved oxidative stress.[64] EPS is mainly composed of protein, polysaccharose, and humic substances.[24,25] Interestingly, the proteins and polysaccharose in EPS are reactive with radicals.[65] The presence of CdS and TiO_2 decreased the polysaccharose content of EPS compared to the control and Fe_2O_3 treatment (Figure S12). The decreased polysaccharose content may have been due to consumption as hole scavengers of CdS or TiO_2 to alleviate ROS damage.[22,64]

Furthermore, our experimental results demonstrated significant increases in protein content in the presence of PNPs. The protein contents play an important role in the three-dimensional structure of biofilm matrix,[25] which is crucial to cell−cell interspecies and intraspecies interactions.[66] The SEM morphology (the green rectangle in Figure S6) showed a loose and porous structure in the control periphytic biofilm and a rough structure in the presence of PNPs. The latter biofilm structure was more favorable to diffuse public good secretion (including allelochemicals) compared to the loose structure of biofilm in the control.[66] Thus, increasing protein content may also contribute to the diffusion of allelochemicals which help to optimize community composition of periphytic biofilm.[15,33] Although the presence of PNPs had a minor negative influence on periphytic biofilm diversity, the relative abundance of beneficial populations increased in periphytic biofilm (phototrophic and high nutrient metabolic microorganisms such as families Chlamydomonadaceae, Cyanobacteriacea, Sphingobacteriales, and Xanthomonadaceae) which may be helpful to produce more EPS. Overall, due to the increasing EPS productivity and population changes, periphytic biofilm was competent to defend itself against intrusion of PNPs.

Prospective Environmental Applications. Recently, researchers have been able to develop combined photocatalytic−biological systems to enhance contaminant removal efficiency.[5] These strategies have been successfully demonstrated by fast biodegradation rates of organic pollutants such as trichlorophenols and dyes.[67,68] Considering the oxidative stress of photocatalysts (especially the PNPs) to organisms, intimately coupled photobiocatalytic processes need complicated reactor configurations to protect microorganisms from being attacked or killed by PNPs or materials with lower toxicity to microorganisms.[5−7] Periphytic biofilm, as a model multispecies microbial aggregate, exhibits constant adaptation of its population fitness to protect microorganisms against PNP stress. This study demonstrated that periphytic biofilm possesses the potential to combine with photocatalysis as periphytic biofilm can maintain its growth in the presence of PNPs. Although periphytic biofilm persists in the presence of PNPs, it is equally important to demonstrate whether it would still maintain the biological treatment function in further research in the future.

DOI: 10.1021/acs.est.8b04923
Environ. Sci. Technol. 2019, 53, 1585−1594

■ ASSOCIATED CONTENT

Supporting Information

The Supporting Information is available free of charge on the ACS Publications website at DOI: 10.1021/acs.est.8b04923.

Periphytic biofilm culture system; composition of the Woods Hole culture medium; measurement of biomass and total chlorophyll content; EPS extraction methods; determination of PNPs distribution in periphytic biofilm system; determination of ROS by electron paramagnetic resonance spectroscopy; measurement of the ROS accumulation; measurement of SOD and ATPase activity; preparation for morphology study; phylogenetic analysis of periphytic biofilm; adsorption assay experimental procedures; table with exposure of periphytic biofilm to photocatalytic nanoparticles (PNPs) with different concentrations (mg L^{-1}); table with hydrodynamic diameters (HD) of PNPs in WC medium or in EPS extract; XRD patterns of PNPs used (CdS, TiO_2, and Fe_2O_3); TEM images of PNPs in WC medium or in EPS extract; intracellular protein content in periphytic biofilm; effects of heat treatment on reactive oxygen species (ROS) accumulation in periphytic biofilm in the presence (CK1) and absence (CK2) of EPS; distribution of PNPs in periphytic biofilm system (in EPS and solution); SEM images of the surface of periphytic biofilm and the corresponding EDS spectra; SEM images of cross-section of periphytic biofilm and the corresponding EDS spectra; TEM images of periphytic biofilm; canonical correspondence analysis (CCA) of the bacterial communities with responses of periphytic biofilm; kinetic adsorption of EPS by PNPs; correlation between EPS productivity and SOD activity; polysaccharose, protein, and humic acid content in EPS of periphytic biofilm in the control and in the presence of PNPs; and references (PDF)

■ AUTHOR INFORMATION

Corresponding Author

*E-mail: tangjun@issas.ac.cn.

ORCID

Jun Tang: 0000-0002-6372-7480
Po Keung Wong: 0000-0003-3081-960X
Dionysios D. Dionysiou: 0000-0002-6974-9197
Yonghong Wu: 0000-0002-2985-219X

Notes

The authors declare no competing financial interest.

■ ACKNOWLEDGMENTS

This work was supported by the National Natural Science Foundation of China (31772396). N.Z. also acknowledgements the support from the UCAS Joint PhD Training Program. This work was also supported by the Scientific Research and Service Platform Fund of Henan Province (2016151) and The Fund of Scientific and Technological Innovation Team of Water Ecological Security for Water Source Region of Midline of South-to-North Diversion Project of Henan Province. D.D.D. also acknowledges support from the University of Cincinnati through a UNESCO co-Chair Professor position on "Water Access and Sustainability" and the Herman Schneider Professorship in the College of Engineering and Applied Sciences.

■ REFERENCES

(1) Maurer-Jones, M. A.; Gunsolus, I. L.; Murphy, C. J.; Haynes, C. L. Toxicity of engineered nanoparticles in the environment. *Anal. Chem.* **2013**, *85* (6), 3036−3049.

(2) Gomes Silva, C.; Juárez, R.; Marino, T.; Molinari, R.; García, H. Influence of excitation wavelength (UV or visible light) on the photocatalytic activity of titania containing gold nanoparticles for the generation of hydrogen or oxygen from water. *J. Am. Chem. Soc.* **2011**, *133* (3), 595−602.

(3) Huckaba, A. J.; Shirley, H.; Lamb, R. W.; Guertin, S.; Autry, S.; Cheema, H.; Talukdar, K.; Jones, T.; Jurss, J. W.; Dass, A.; Hammer, N. I.; Schmehl, R. H.; Webster, C. E.; Delcamp, J. H. A mononuclear tungsten photocatalyst for H_2 production. *ACS Catal.* **2018**, *8* (6), 4838−4847.

(4) Qu, Y. Q.; Duan, X. F. Progress, challenge and perspective of heterogeneous photocatalysts. *Chem. Soc. Rev.* **2013**, *42* (7), 2568−2580.

(5) Rittmann, B. E. Biofilms, active substrata, and me. *Water Res.* **2018**, *132*, 135−145.

(6) Tang, Y. X.; Zhang, Y. M.; Yan, N.; Liu, R.; Rittmann, B. E. The role of electron donors generated from UV photolysis for accelerating pyridine biodegradation. *Biotechnol. Bioeng.* **2015**, *112* (9), 1792−1800.

(7) Qian, F.; Wang, H.; Ling, Y.; Wang, G.; Thelen, M. P.; Li, Y. Photoenhanced electrochemical interaction between *Shewanella* and a hematite nanowire photoanode. *Nano Lett.* **2014**, *14* (6), 3688−3693.

(8) Wu, W.; Jiang, C. Z.; Roy, V. A. L. Recent progress in magnetic iron oxide-semiconductor composite nanomaterials as promising photocatalysts. *Nanoscale* **2015**, *7* (1), 38−58.

(9) Kubacka, A.; Fernández-García, M.; Colón, G. Advanced nanoarchitectures for solar photocatalytic applications. *Chem. Rev.* **2012**, *112* (3), 1555−1614.

(10) Brown, K. A.; Harris, D. F.; Wilker, M. B.; Rasmussen, A.; Khadka, N.; Hamby, H.; Keable, S.; Dukovic, G.; Peters, J. W.; Seefeldt, L. C.; King, P. W. Light-driven dinitrogen reduction catalyzed by a CdS: nitrogenase MoFe protein biohybrid. *Science* **2010**, *352* (6284), 448−450.

(11) Zhang, L. S.; Wong, K. H.; Yip, H. Y.; Hu, C.; Yu, J. C.; Chan, C. Y.; Wong, P. K. Effective photocatalytic disinfection of *E. coli K-12* using AgBr-Ag-Bi_2WO_6 nanojunction system irradiated by visible light: The role of diffusing hydroxyl radicals. *Environ. Sci. Technol.* **2010**, *44* (4), 1392−1398.

(12) Polo-López, M. I.; Castro-Alférez, M.; Oller, I.; Fernández-Ibáñez, P. Assessment of solar photo-Fenton, photocatalysis, and H_2O_2 for removal of phytopathogen fungi spores in synthetic and real effluents of urban wastewater. *Chem. Eng. J.* **2014**, *257*, 122−130.

(13) Song, J.; Wang, X.; Ma, J.; Wang, X.; Wang, J.; Xia, S.; Zhao, J. Removal of *Microcystis aeruginosa* and Microcystin-LR using a graphitic-C_3N_4/TiO_2 floating photocatalyst under visible light irradiation. *Chem. Eng. J.* **2018**, *348*, 380−388.

(14) Gil-Allué, C.; Tlili, A.; Schirmer, K.; Gessner, M. O.; Behra, R. Long-term exposure to silver nanoparticles affects periphyton community structure and function. *Environ. Sci.: Nano* **2018**, *5* (6), 1397−1407.

(15) Tang, J.; Zhu, N.; Zhu, Y.; Liu, J.; Wu, C.; Kerr, P.; Wu, Y.; Lam, P. K. S. Responses of periphyton to Fe_2O_3 nanoparticles: A physiological and ecological basis for defending nanotoxicity. *Environ. Sci. Technol.* **2017**, *51* (18), 10797−10805.

(16) Miao, L.; Wang, P.; Wang, C.; Hou, J.; Yao, Y.; Liu, J.; Lv, B.; Yang, Y.; You, G.; Xu, Y.; Liu, Z.; Liu, S. Effect of TiO_2 and CeO_2 nanoparticles on the metabolic activity of surficial sediment microbial communities based on oxygen microelectrodes and high-throughput sequencing. *Water Res.* **2018**, *129*, 287−296.

(17) Tang, J.; Zhu, N.; Zhu, Y.; Kerr, P.; Wu, Y. Distinguishing the roles of different extracellular polymeric substance fractions of a periphytic biofilm in defending against Fe_2O_3 nanoparticle toxicity. *Environ. Sci.: Nano* **2017**, *4* (8), 1682−1691.

(18) Ferry, J. L.; Craig, P.; Hexel, C.; Sisco, P.; Frey, R.; Pennington, P. L.; Fulton, M. H.; Scott, I. G.; Decho, A. W.; Kashiwada, S.;

DOI: 10.1021/acs.est.8b04923
Environ. Sci. Technol. 2019, 53, 1585−1594

Murphy, C. J.; Shaw, T. J. Transfer of gold nanoparticles from the water column to the estuarine food web. *Nat. Nanotechnol.* **2009**, *4*, 441−444.
(19) Avellan, A.; Simonin, M.; McGivney, E.; Bossa, N.; Spielman-Sun, E.; Rocca, J. D.; Bernhardt, E. S.; Geitner, N. K.; Unrine, J. M.; Wiesner, M. R.; Lowry, G. V. Gold nanoparticle biodissolution by a freshwater macrophyte and its associated microbiome. *Nat. Nanotechnol.* **2018**, *13*, 1072−1077.
(20) Baudrimont, M.; Andrei, J.; Mornet, S.; Gonzalez, P.; Mesmer-Dudons, N.; Gourves, P. Y.; Jaffal, A.; Dedourge-Geffard, O.; Geffard, A.; Geffard, O.; Garric, J.; Feurtet-Mazel, A. Trophic transfer and effects of gold nanoparticles (AuNPs) in *Gammarus fossarum* from contaminated periphytic biofilm. *Environ. Sci. Pollut. Res.* **2018**, *25* (12), 11181−11191.
(21) Zhu, N.; Zhang, J.; Tang, J.; Zhu, Y.; Wu, Y. Arsenic removal by periphytic biofilm and its application combined with biochar. *Bioresour. Technol.* **2018**, *248* (B), 49−55.
(22) Zhu, N.; Wu, Y.; Tang, J.; Duan, P.; Yao, L.; Rene, E. R.; Wong, P. K.; An, T.; Dionysiou, D. D. A new concept of promoting nitrate reduction in surface waters: simultaneous supplement of denitrifiers, electron donor pool and electron mediators. *Environ. Sci. Technol.* **2018**, *52* (15), 8617−8626.
(23) Zhu, N.; Tang, J.; Tang, C.; Duan, P.; Yao, L.; Wu, Y.; Dionysiou, D. D. Combined CdS nanoparticles-assisted photocatalysis and periphytic biological processes for nitrate removal. *Chem. Eng. J.* **2018**, *353*, 237−245.
(24) Stewart, T. J.; Behra, R.; Sigg, L. Impact of chronic lead exposure on metal distribution and biological effects to periphyton. *Environ. Sci. Technol.* **2015**, *49* (8), 5044−5051.
(25) Flemming, H. C.; Wingender, J. The biofilm matrix. *Nat. Rev. Microbiol.* **2010**, *8* (9), 623−633.
(26) Roder, H. L.; Sorensen, S. J.; Burmolle, M. Studying bacterial multispecies biofilms: Where to start? *Trends Microbiol.* **2016**, *24* (6), 503−513.
(27) Echavarri-Bravo, V.; Paterson, L.; Aspray, T. J.; Porter, J. S.; Winson, M. K.; Thornton, B.; Hartl, M. G. J. Shifts in the metabolic function of a benthic estuarine microbial community following a single pulse exposure to silver nanoparticles. *Environ. Pollut.* **2015**, *201*, 91−99.
(28) Ganguly, P.; Byrne, C.; Breen, A.; Pillai, S. C. Antimicrobial activity of photocatalysts: Fundamentals, mechanisms, kinetics and recent advances. *Appl. Catal., B* **2018**, *225*, 51−75.
(29) Zhang, H. Y.; Ji, Z. X.; Xia, T.; Meng, H.; Low-Kam, C.; Liu, R.; Pokhrel, S.; Lin, S. J.; Wang, X.; Liao, Y. P.; Wang, M. Y.; Li, L. J.; Rallo, R.; Damoiseaux, R.; Telesca, D.; Madler, L.; Cohen, Y.; Zink, J. I.; Nel, A. E. Use of metal oxide nanoparticle band gap to develop a predictive paradigm for oxidative stress and acute pulmonary inflammation. *ACS Nano* **2012**, *6* (5), 4349−4368.
(30) Saleh, N. B.; Milliron, D. J.; Aich, N.; Katz, L. E.; Liljestrand, H. M.; Kirisits, M. J. Importance of doping, dopant distribution, and defects on electronic band structure alteration of metal oxide nanoparticles: Implications for reactive oxygen species. *Sci. Total Environ.* **2016**, *568*, 926−932.
(31) Kaweeteerawat, C.; Ivask, A.; Liu, R.; Zhang, H.; Chang, C. H.; Low-Kam, C.; Fischer, H.; Ji, Z.; Pokhrel, S.; Cohen, Y.; Telesca, D.; Zink, J.; Maedler, L.; Holden, P. A.; Nel, A.; Godwin, H. Toxicity of metal oxide nanoparticles in *Escherichia coli* correlates with conduction band and hydration energies. *Environ. Sci. Technol.* **2015**, *49* (2), 1105−1112.
(32) Noventa, S.; Hacker, C.; Rowe, D.; Elgy, C.; Galloway, T. Dissolution and bandgap paradigms for predicting the toxicity of metal oxide nanoparticles in the marine environment: an in vivo study with oyster embryos. *Nanotoxicology* **2018**, *12* (1), 63−78.
(33) Wu, Y.; Liu, J.; Yang, L.; Chen, H.; Zhang, S.; Zhao, H.; Zhang, N. Allelopathic control of cyanobacterial blooms by periphyton biofilms. *Environ. Microbiol.* **2011**, *13* (3), 604−615.
(34) Jing, Z.; Chen, R.; Wei, S.; Feng, Y.; Zhang, J.; Lin, X. Response and feedback of C mineralization to P availability driven by soil microorganisms. *Soil Biol. Biochem.* **2017**, *105*, 111−120.
(35) Lin, D.; Drew Story, S.; Walker, S. L.; Huang, Q.; Cai, P. Influence of extracellular polymeric substances on the aggregation kinetics of TiO_2 nanoparticles. *Water Res.* **2016**, *104*, 381−388.
(36) Li, C.; Sun, Z.; Zhang, W.; Yu, C.; Zheng, S. Highly efficient g-C_3N_4/TiO_2/kaolinite composite with novel three-dimensional structure and enhanced visible light responding ability towards *Ciprofloxacin* and *S. aureus*. *Appl. Catal., B* **2018**, *220*, 272−282.
(37) Jeong, M. S.; Yu, K. N.; Chung, H. H.; Park, S. J.; Lee, A. Y.; Song, M. R.; Cho, M. H.; Kim, J. S. Methodological considerations of electron spin resonance spin trapping techniques for measuring reactive oxygen species generated from metal oxide nanomaterials. *Sci. Rep.* **2016**, *6*, 26347 DOI: 10.1038/srep26347.
(38) Wang, C.; Huang, Z. Controlled synthesis of α-Fe_2O_3 nanostructures for efficient photocatalysis. *Mater. Lett.* **2016**, *164*, 194−197.
(39) Tu, W.; Zhou, Y.; Zou, Z. Versatile graphene-promoting photocatalytic performance of semiconductors: basic principles, synthesis, solar energy conversion, and environmental applications. *Adv. Funct. Mater.* **2013**, *23* (40), 4996−5008.
(40) Breker, M.; Schuldiner, M. The emergence of proteome-wide technologies: systematic analysis of proteins comes of age. *Nat. Rev. Mol. Cell Biol.* **2014**, *15* (7), 453−464.
(41) Venieri, D.; Gounaki, I.; Bikouvaraki, M.; Binas, V.; Zachopoulos, A.; Kiriakidis, G.; Mantzavinos, D. Solar photocatalysis as disinfection technique: Inactivation of *Klebsiella pneumoniae* in sewage and investigation of changes in antibiotic resistance profile. *J. Environ. Manage.* **2017**, *195*, 140−147.
(42) Abreu, I. A.; Cabelli, D. E. Superoxide dismutases-a review of the metal-associated mechanistic variations. *Biochim. Biophys. Acta, Proteins Proteomics* **2010**, *1804* (2), 263−274.
(43) Seaver, L. C.; Imlay, J. A. Are respiratory enzymes the primary sources of intracellular hydrogen peroxide? *J. Biol. Chem.* **2004**, *279* (47), 48742−48750.
(44) Castro-Alférez, M.; Polo-López, M. I.; Marugán, J.; Fernández-Ibáñez, P. Mechanistic model of the *Escherichia coli* inactivation by solar disinfection based on the photo-generation of internal ROS and the photo-inactivation of enzymes: CAT and SOD. *Chem. Eng. J.* **2017**, *318*, 214−223.
(45) Yang, Y.; Nie, X.; Jiang, Y.; Yang, C.; Gu, Y.; Jiang, W. Metabolic regulation in solventogenic clostridia: regulators, mechanisms and engineering. *Biotechnol. Adv.* **2018**, *36* (4), 905−914.
(46) Bhatnagar, M.; Parwani, L.; Sharma, V.; Ganguly, J.; Bhatnagar, A. Exopolymers from Tolypothrix tenuis and three *Anabaena sp. (Cyanobacteriaceae)* as novel blood clotting agents for wound management. *Carbohydr. Polym.* **2014**, *99*, 692−699.
(47) Mark Ibekwe, A.; Murinda, S. E.; Murry, M. A.; Schwartz, G.; Lundquist, T. Microbial community structures in high rate algae ponds for bioconversion of agricultural wastes from livestock industry for feed production. *Sci. Total Environ.* **2017**, *580*, 1185−1196.
(48) Srivastava, V.; Gusain, D.; Sharma, Y. C. Critical review on the toxicity of some widely used engineered nanoparticles. *Ind. Eng. Chem. Res.* **2015**, *54* (24), 6209−6233.
(49) Joris, F.; Manshian, B. B.; Peynshaert, K.; De Smedt, S. C.; Braeckmans, K.; Soenen, S. J. Assessing nanoparticle toxicity in cell-based assays: influence of cell culture parameters and optimized models for bridging the *in vitro-in vivo* gap. *Chem. Soc. Rev.* **2013**, *42* (21), 8339−59.
(50) Karunakaran, G.; Jagathambal, M.; Gusev, A.; Kolesnikov, E.; Kuznetsov, D. Assessment of FeO and MnO nanoparticles toxicity on *Chlorella pyrenoidosa*. *J. Nanosci. Nanotechnol.* **2017**, *17* (3), 1712−1720.
(51) Niazi, J. H.; Gu, M. B. Toxicity of metallic nanoparticles in microorganisms- a review. In *Atmospheric and Biological Environmental Monitoring*; Kim, Y. J., Platt, U., Gu, M. B., Iwahashi, H., Eds.; Springer: Dordrecht, Netherlands, 2009; pp 193−206.
(52) Biswaro, L. S.; Sousa, M. G. D.; Rezende, T. M. B.; Dias, S. C.; Franco, O. L. Antimicrobial peptides and nanotechnology, recent advances and challenges. *Front. Microbiol.* **2018**, *9*, 14.

DOI: 10.1021/acs.est.8b04923
Environ. Sci. Technol. 2019, 53, 1585−1594

(53) Poynton, H. C.; Lazorchak, J. M.; Impellitteri, C. A.; Blalock, B. J.; Rogers, K.; Allen, H. J.; Loguinov, A.; Heckman, J. L.; Govindasmawy, S. Toxicogenomic responses of nanotoxicity in *Daphnia magna* exposed to silver nitrate and coated silver nanoparticles. *Environ. Sci. Technol.* **2012**, *46* (11), 6288−6296.
(54) Zhang, L.; Li, J.; Yang, K.; Liu, J.; Lin, D. Physicochemical transformation and algal toxicity of engineered nanoparticles in surface water samples. *Environ. Pollut.* **2016**, *211*, 132−140.
(55) Rtimi, S.; Pulgarin, C.; Robyr, M.; Aybush, A.; Shelaev, I.; Gostev, F.; Nadtochenko, V.; Kiwi, J. Insight into the catalyst/photocatalyst microstructure presenting the same composition but leading to a variance in bacterial reduction under indoor visible light. *Appl. Catal., B* **2017**, *208*, 135−147.
(56) Zengler, K.; Zaramela, L. S. The social network of microorganisms - how auxotrophies shape complex communities. *Nat. Rev. Microbiol.* **2018**, *16* (6), 383−390.
(57) Zhu, N.; Yan, T.; Qiao, J.; Cao, H. Adsorption of arsenic, phosphorus and chromium by bismuth impregnated biochar: Adsorption mechanism and depleted adsorbent utilization. *Chemosphere* **2016**, *164*, 32−40.
(58) Lin, D.; Story, S. D.; Walker, S. L.; Huang, Q.; Liang, W.; Cai, P. Role of pH and ionic strength in the aggregation of TiO_2 nanoparticles in the presence of extracellular polymeric substances from *Bacillus subtilis*. *Environ. Pollut.* **2017**, *228*, 35−42.
(59) Burello, E.; Worth, A. P. A theoretical framework for predicting the oxidative stress potential of oxide nanoparticles. *Nanotoxicology* **2011**, *5* (2), 228−235.
(60) Xu, Y.; Schoonen, M. A. A. The absolute energy positions of conduction and valence bands of selected semiconducting minerals. *Am. Mineral.* **2000**, *85* (3−4), 543−556.
(61) He, W.; Jia, H.; Wamer, W. G.; Zheng, Z.; Li, P.; Callahan, J. H.; Yin, J. J. Predicting and identifying reactive oxygen species and electrons for photocatalytic metal sulfide micro−nano structures. *J. Catal.* **2014**, *320*, 97−105.
(62) Op De Beeck, M.; Troein, C.; Peterson, C.; Persson, P.; Tunlid, A. Fenton reaction facilitates organic nitrogen acquisition by an ectomycorrhizal fungus. *New Phytol.* **2018**, *218* (1), 335−343.
(63) Desmond, P.; Best, J. P.; Morgenroth, E.; Derlon, N. Linking composition of extracellular polymeric substances (EPS) to the physical structure and hydraulic resistance of membrane biofilms. *Water Res.* **2018**, *132*, 211−221.
(64) Han, X. M.; Wang, Z. W.; Chen, M.; Zhang, X. R.; Tang, C. Y.; Wu, Z. C. Acute responses of microorganisms from membrane bioreactors in the presence of NaOCl: Protective mechanisms of extracellular polymeric substances. *Environ. Sci. Technol.* **2017**, *51* (6), 3233−3241.
(65) Coburn, K. M.; Wang, Q. Z.; Rediske, D.; Viola, R. E.; Hanson, B. L.; Xue, Z.; Seo, Y. Effects of extracellular polymeric substance composition on bacteria disinfection by monochloramine: application of MALDI-TOF/TOE-MS and multivariate analysis. *Environ. Sci. Technol.* **2016**, *50* (17), 9197−9205.
(66) Nadell, C. D.; Drescher, K.; Foster, K. R. Spatial structure, cooperation and competition in biofilms. *Nat. Rev. Microbiol.* **2016**, *14* (9), 589−600.
(67) Li, G. Z.; Park, S.; Rittmann, B. E. Developing an efficient TiO_2-coated biofilm carrier for intimate coupling of photocatalysis and biodegradation. *Water Res.* **2012**, *46* (19), 6489−6496.
(68) Li, G. Z.; Park, S.; Kang, D. W.; Krajmalnik-Brown, R.; Rittmann, B. E. 2,4,5-Trichlorophenol degradation using a novel TiO_2-coated biofilm carrier: Roles of adsorption, photocatalysis, and biodegradation. *Environ. Sci. Technol.* **2011**, *45* (19), 8359−8367.

DOI: 10.1021/acs.est.8b04923
Environ. Sci. Technol. 2019, 53, 1585−1594